Nat. Hazards Earth Syst. Sci. Discuss., 2, 2813–2849, 2014
www.nat-hazards-earth-syst-sci-discuss.net/2/2813/2014/
doi:10.5194/nhessd-2-2813-2014
© Author(s) 2014. CC Attribution 3.0 License.

Natural Hazards and Earth System Sciences
Open Access
Discussions

This discussion paper is/has been under review for the journal Natural Hazards and Earth System Sciences (NHESS). Please refer to the corresponding final paper in NHESS if available.

Non-susceptible landslide areas in Italy and in the Mediterranean region

I. Marchesini[1], F. Ardizzone[1], M. Alvioli[1], M. Rossi[1,2], and F. Guzzetti[1]

[1]Consiglio Nazionale delle Ricerche, Istituto di Ricerca per la Protezione Idrogeologica, via Madonna Alta 126, 06128 Perugia, Italy
[2]Università degli Studi di Perugia, Dipartimento di Scienze della Terra, Piazza Università, 1, 06123, Perugia, Italy

Received: 9 January 2014 – Accepted: 6 April 2014 – Published: 24 April 2014

Correspondence to: I. Marchesini (ivan.marchesini@irpi.cnr.it)

Published by Copernicus Publications on behalf of the European Geosciences Union.

Abstract

We used landslide information for 13 study areas in Italy and morphometric information obtained from the 3 arc-second SRTM DEM to determine areas where landslide susceptibility is expected to be null or negligible in Italy, and in the landmasses surrounding the Mediterranean Sea. The morphometric information consisted in the local terrain slope computed in a square 3 × 3 cell moving window, and in the regional relative relief computed in a circular 15 × 15 cell moving window. We tested three different models to determine the non-susceptible landslide areas, including a linear model (LR), a quantile linear model (QLR), and a quantile non-linear model (QNL). We tested the performance of the three models using independent landslide information represented by the Italian Landslide Inventory (*Inventario Fenomeni Franosi in Italia – IFFI*). Best results were obtained using the QNL model. The corresponding zonation of non-susceptible landslide areas was intersected in a GIS with geographical census data for Italy. The result allowed determining that 57.5 % of the population of Italy (in 2001) was located in areas where landslide susceptibility is expected to be null or negligible, and that the remaining 42.5 % was located in areas where some landslide susceptibility is expected. We applied the QNL model to the landmasses surrounding the Mediterranean Sea, and we tested the synoptic non-susceptibility zonation using independent landslide information for three study areas in Spain. Results proved that the QNL model was capable of determining where landslide susceptibility is expected to be negligible in the Mediterranean area. We expect our results to be applicable in similar study areas, facilitating the identification of non-susceptible and susceptible landslide areas, at the synoptic scale.

1 Introduction

Landslide susceptibility is the likelihood of a landslide occurring in a given area (Brabb, 1984). It is an estimate of "where" landslides are expected to occur on the basis of local

NHESSD
2, 2813–2849, 2014

geo-environmental conditions (Guzzetti, 2005). Over the past three decades, research scientists, and planning and environmental organisations have attempted – with various degrees of success – to assess landslide susceptibility at different geographical scales, and to produce maps portraying its spatial distribution (i.e., landslide susceptibility zonations). A large number of methods and techniques were proposed and tested to ascertain landslide susceptibility, including geomorphological mapping, analysis of inventories, heuristic zoning, statistical and probabilistic methods, and process-based (conceptual) models, using a variety of mapping units, including grid cells, terrain units, unique condition units, slope units, geo-hydrological units, topographic units, and geographical (administrative) units (Guzzetti et al., 1999; Guzzetti, 2005). In the recent years, a few attempts were made to determine landslide susceptibility at the continental and even at the global scale (Nadim et al., 2006; Hong et al., 2007a, b; Kirschbaum et al., 2009; Van Den Eeckhaut et al., 2012; Farahmand and AghaKouchak, 2013; Gunther et al., 2013). Due to the generalised lack of accurate and complete landslide information (Guzzetti et al., 2012), these synoptic scale attempts have either not used information on the location and extent of the landslides, or have used unsystematic point landslide information to ascertain landslide susceptibility (Gunther et al., 2013).

Regardless of the mapping unit and the method used, all the proposed attempts focus – directly or indirectly, and explicitly or implicitly – on the identification of the areas where susceptibility is expected to be largest i.e., on the definition of the potentially most hazardous landslide areas (Chung and Fabbri, 1999; Guzzetti et al., 1999, 2005a). Little effort was made to determine where landslides are not expected i.e., where landslide susceptibility is null, or negligible (Chung and Fabbri, 2003; Fabbri et al., 2003; Godt et al., 2012). A notable exception is the work of Godt et al. (2012), who have proposed a synoptic map for the conterminous United States showing areas with negligible landslide susceptibility, i.e., areas where landslides are not expected.

In this work, we propose a method for the definition of non-susceptible landslide areas, at the synoptic scale. To construct the method, we use accurate landslide information for 13 areas in Italy. We apply the method in Italy and to the landmasses

NHESSD
2, 2813–2849, 2014

surrounding the Mediterranean Sea (Fig. 1) obtaining synoptic-scale maps showing areas where landslides are not expected in Italy and in the Mediterranean area.

2 Available data and preliminary processing

For our study, we used digital terrain elevation and landslide information.

2.1 Terrain information

The terrain elevation data consisted in the Shuttle Radar Topography Mission (SRTM) version 2.1 Digital Elevation Model (DEM), available from http://dds.cr.usgs.gov/srtm/ (Jarvis et al., 2009; Farr et al., 2007; Verdin et al., 2007). In the DEM, elevation data have a 3 arc-second ground spacing in latitude and longitude, approximately 92 m × 92 m at the equator and 92 m × 69 m at the latitudes of our study areas. The DEM is distributed in 5° × 5° tiles, in the WGS84 (EPSG 4326) longitude-latitude Coordinate Reference System (CRS). Following Godt et al. (2012), we maintained the DEM in the original geographical (latitude, longitude) CRS, and we assembled eight tiles to cover the Italian territory, and 40 tiles to cover the Mediterranean area (Fig. 1).

2.2 Landslide information

The landslide information was obtained from 13 geomorphological (Antonini et al., 1993, 2000; Cardinali et al., 2001; Antonini et al., 2002), event (Cardinali et al., 2000; Guzzetti et al., 2004; Ardizzone et al., 2007, 2012), and multi-temporal (Guzzetti et al., 2005a, 2006, 2009; Galli et al., 2008) inventory maps in Italy (Fig. 2). The individual landslide maps cover areas ranging from 19 to 9366 km^2, and were prepared in the period from 1993 to 2013 by the same general team of geomorphologists (http://geomorphology.irpi.cnr.it) through the visual interpretation of stereoscopic aerial photographs flown at scales ranging from 1 : 5000 to 75 000, aided by field checks carried out primarily after meteorological landslide triggering events (Cardinali et al., 2000;

NHESSD
2, 2813–2849, 2014

Guzzetti et al., 2004; Ardizzone et al., 2012), or to validate locally the geomorphological (Antonini et al., 1993, 2000, 2002; Cardinali et al., 2001) and the multitemporal (Guzzetti et al., 2005a, 2006, 2009; Galli et al., 2008) inventories. The landslide information obtained from the aerial photographs or in the field was transferred, visually or using semi-automatic methods, on topographic base maps at scales ranging from 1 : 10 000 to 1 : 25 000. The base maps were in different CRSs, including the Gauss Boaga West (EPSG 3003) and East (EPSG 3004) CRSs, and the Zone 32 (EPSG 23032) and Zone 33 (EPSG 23033) UTM-ED50 CRSs. The landslide information was then digitized, and stored in dedicated GIS databases where the individual landslides are shown by polygons, in vector format. For our analyses, we first transformed the landslide information from their original CRS to the WGS84 (EPSG 4326) longitude-latitude CRS, for consistency with the the CRS used by the SRTM-DEM. Next, we transformed the vector landslide information to a raster (grid) format.

Collectively, the 13 inventories are representative of most of the physiographical provinces in Italy (Guzzetti and Reichenbach, 1994) where landslides are abundant (Fig. 2). Figure 3 summarises the distributions of terrain elevation and slope in the 13 study areas, and Table 1 lists the main characteristics of the landslide inventory maps. Collectively, the 13 landslide maps cover 26 992 km^2 (8.9 % of the Italian territory) and show 93 538 landslides, for a total landslide area of 2726 km^2, 10.1 % of the total mapped areas. The inventories show primarily rotational and translational slides, earth flows, and complex and compound movements (Cruden and Varnes, 1996). For some inventories, soil slips, debris flows, rock falls and topples are also sown. We consider these 13 inventories as a significant and consistent statistical sample to describe the topography where landslide are likely to occur.

3 Methods

We determined the areas that are expected to be non susceptible to landslides in Italy, using two different methods. The first method is derived from the work of Godt

NHESSD
2, 2813–2849, 2014

et al. (2012) (method I). The second method was developed specifically for this work (method II). Both methods exploit the landslide information obtained from the available inventory maps (Fig. 2 and Table 1), and two topographic indexes computed from the SRTM DEM i.e., relative relief R (in meters) and terrain slope S (in degrees).

To compute R, we used the `r.neighbors` module of GRASS GIS. The size of the moving window was decided to be consistent with the method of Godt et al. (2012) for the conterminous United States.

We computed R in a 15×15 cell circular moving window and S in a 3×3 cell square moving window. Use of kernels of significantly different sizes captured different morphometric characteristics of the landscape, and reduced the collinearity between the two terrain variables.

Computation of terrain slope S was more demanding, because the SRTM DEM was in geographical coordinates. We computed S in the original latitude-longitude coordinates. For the purpose, we calculated the width of each grid cell in the EW (longitude, $\delta x_{i,j}$), and the NS (latitude, $\delta y_{i,j}$) directions. Denoting $\delta x_0 = \frac{2\pi a \delta\theta}{360}$ the size of a $\delta\theta$-by-$\delta\theta$-degree cell, $a = 6\,378\,137.0000$ m the major axis and $b = 6\,356\,752.3142$ m the minor axis of the WGS84 ellipsoid (corresponding to a flattening ratio $f = 1/298.257223563$ and eccentricity $e^2 = (a^2 - b^2)/a^2$), we calculated the size of each cell as a function of the local latitude $\theta_{i,j}$ as:

$$\delta x_{i,j} = \delta x_0 \cos\theta_{i,j}\,, \tag{1}$$

$$\delta y_{i,j} = \frac{a(1-e^2)}{\left(1 - e^2 \sin^2\theta_{i,j}\right)^{3/2}}\delta\theta\,. \tag{2}$$

NHESSD
2, 2813–2849, 2014

Using the above definitions, we calculated the slope $S_{i,j}$ in the ith row, jth column cell as:

$$S_{i,j} = \arctan\left(\left(\frac{\delta z_{i,j}}{\delta x_{i,j}}\right)^2 + \left(\frac{\delta z_{i,j}}{\delta y_{i,j}}\right)^2\right)^{1/2}, \quad (3)$$

where $z_{i,j}$ is the local terrain elevation and, according to Horn (1981),

$$\frac{\delta z_{i,j}}{\delta x_{i,j}} = \frac{(z_{i+1,j+1} + 2z_{i+1,j} + z_{i+1,j-1}) - (z_{i-1,j+1} + 2z_{i-1,j} + z_{i-1,j-1})}{8\delta x_{i,j}} \quad (4)$$

and

$$\frac{\delta z_{i,j}}{\delta y_{i,j}} = \frac{(z_{i+1,j+1} + 2z_{i,j+1} + z_{i-1,j+1}) - (z_{i+1,j-1} + 2z_{i,j-1} + z_{i-1,j-1})}{8\delta y_{i,j}}. \quad (5)$$

3.1 Method I

Method I modifies slightly the approach proposed by Godt et al. (2012). These authors highlighted that landslide potential is controlled by topography. When dealing with the landslide susceptibility assessment over large areas, the lack of detailed thematic information is critical and makes impossible the use of complex landslide statistical susceptibility models. For such large areas, only simplified susceptibility models based on variables derived from low to medium resolution Digital Elevation Models are suitable. For such reason Godt et al. (2012) arbitrarily chose the 10 % cumulative frequency of both topographic slope and relief as the boundary between "negligible" and "some" landslide susceptibility. The rationale in their approach is that the fitting of these bivariate values is assumed as a critical threshold below which territory has "negligible" susceptibility to landslides (i.e. zones with relatively low values of slope angle and relief are assumed stable). Godt et al. (2012) used an aggregate of 16 000 landslide point

NHESSD
2, 2813–2849, 2014

locations obtained from inventories prepared at different scales for five geographical areas in the conterminous United States (New Mexico, New Jersey, Oregon, California, North Carolina). The landslide information available to us in Italy consisted of polygons showing the location, shape, and size of the individual landslides. The area information is superior to the point information used by Godt et al. (2012), and we exploited the additional information. First, we computed the frequency distribution of the relative relief R and of the terrain slope S for all the grid cells in each single landslide in an inventory.

Next, for each inventory, we prepared Empirical Cumulative Distribution Functions (ECDFs) for the 50th percentile (median) of the two terrain variables, R and S, in all the mapped landslides. As an example, Fig. 4 shows the ECDFs of the median (50th percentile, red line), and the 5th, 25th, 75th, and 95th percentiles of R and S for all the landslides shown in the Valseriana inventory (L in Fig. 2 and Table 1). Figure 5 show the ECDFs of the median of R and S for all the investigated inventories.

Lastly, for each inventory, we selected the 5th percentile of the ECDFs of the median of relative relief R and terrain slope S (Fig. 5), and we plotted the 13 (R_{50}, S_{50}) pairs in a single plot (Fig. 6). We selected the 5th percentile as a reasonable lower threshold to separate between "negligible" and "some" landslide susceptibility (Godt et al., 2012). Inspection of Fig. 6 reveals that the 13 data points (R_{50}, S_{50}) align along a linear trend. We fit the data points with a linear regression model to obtain:

$$S_{50} = 3.448 + 0.040 R_{50} \quad (0 < R_{50} < 350\,\text{m},\ 0 < S < 18^{\circ}), \tag{6}$$

with a residual standard error $R_{SE} = 1.126^{\circ}$.

We used the linear model LR represented by Eq. (6) to prepare the binary zonation of the Italian territory shown in maps I of Fig. 7. In the map, the red (non-susceptible) areas are areas where landslide susceptibility is expected to be null or negligible. The other areas are areas where some susceptibility is expected (Godt et al., 2012). The non-susceptible areas are characterized by (R_{50}, S_{50}) pairs below or equal to the LR model, and the susceptible areas are characterized by (R_{50}, S_{50}) pairs above the LR model.

NHESSD
2, 2813–2849, 2014

3.2 Method II

For the second method, we used all the values of relative relief R and terrain slope S computed for all the grid cells (3 arc-second resolution) in all the landslide polygons shown in the 13 inventory maps. Where overlapping inventories exists (see Fig. 2), we used only the most detailed inventory. In particular, the Upper Tiber River inventory (C in Table 1) was used where it does not overlap with the Umbria inventory (A in Table 1), and the Collazone inventory (C in Table 1) was preferred to the Umbria inventory in the overlapping area.

We plotted the 354 406 (R, S) pairs in Fig. 8, and we searched for a lower threshold to the cloud of empirical data points. To determine the lower threshold, we performed a quantile regression (Koenker, 2005) testing linear (QLR) and non linear (exponential) (QNL) models. We instructed the quantile regression to search for a 5 % lower boundary i.e., for a regression line that would leave below the line 5 % of the empirical data points. Quantile regression model (QLR) resulted in the function:

$$S = 0.245 + 0.032R \quad (0 < R < 1000\,\text{m},\ 0 < S < 70^\circ), \tag{7}$$

with a residual standard error $R_{SE} = 7.970^\circ$.

Quantile regression of a non linear model (QNL) resulted in the exponential function:

$$S = 3.539\exp(0.0028 \times R) \quad (0 < R < 1000\,\text{m},\ 0 < S < 70^\circ), \tag{8}$$

with a residual standard error $R_{SE} = 8.534^\circ$.

We checked the proportion of empirical data points below the QLR and the QNL threshold models, and found that the linear model QLR leaves 5.0 % of the empirical points below the threshold, and the exponential model QNL leaves 5.3 % of the empirical points below the threshold. Considering the large dispersion of in the empirical data (Fig. 8), we consider the two models QLR and QNL substantially equivalent in their ability to leave the prescribed number of points below the model threshold line. We further observe that the QNL exponential model predicts a "negligible" landslide

NHESSD
2, 2813–2849, 2014

susceptibility where $S < 3.5^{\circ}$, regardless of the regional relative relief, and the QLR linear model predicts a negligible landslide susceptibility for $S < 0.3^{\circ}$.

We used the linear model QLR represented by Eq. (7) and the non linear model QNL represented by Eq. (8) to prepare two alternative binary zonations showing non-susceptible and susceptible landslide areas in Italy. Results are shown in Figs. 7II and 7III, respectively.

4 Models performance

To select the most appropriate model for the definition of non-susceptible landslide areas in Italy, we tested the three models (represented in maps I, II and III of Fig. 7) against independent landslide information. For the purpose, we used the Italian Landslide Inventory (*Inventario Fenomeni Franosi in Italia – IFFI*), the single largest collection of landslide information in Italy (Trigila et al., 2010). Specifically, we used the IFFI geographical database available through a Web Map Service (WMS) offered by the *Istituto Superiore per la Protezione e la Ricerca Ambientale – ISPRA*. According to Trigila et al. (2010), IFFI shows some inconsistencies and lack of homogeneity of the landslide data due to the different levels of detail of the used previously existing inventories. Moreover the quality of the inventory is affected by the greater or lesser degree of use of the aerial photo interpretation, field surveys, or historical and archives data in the methodology adopted by the individual Regions/Self-Governing Provinces. Due to aforementioned problems we decided to use IFFI just in the validation phase, and our detailed and consistent inventories to train the non-susceptibility statistical models.

To obtain the landslide information, we performed tiled "GetMap" requests to the WMS service (De La Beaujardiere, 2004). As a compromise between geographical accuracy of the landslide information and time required for the requests, we have set a ground resolution equivalent to 5 m × 5 m for the landslide information. We retrieved only information on landslides shown as polygons in the IFFI geographical database, discarding landslides represented by points and linear features. We also discarded

NHESSD
2, 2813–2849, 2014

areas classified as "*affected by diffused landslides*" in the IFFI database. Each request resulted in a single Portable Network Graphics (PNG) file. We assembled all the PNG files in a single raster layer where the landslide types were separated on the basis of the colour of the individual landslides. In the GIS layer, landslides were classified as fall and/or topple (2.83 % of the total landslide cells), slow flow (17.73 %), rapid flow (5.07 %), complex movement (34.85 %), rotational/translational slide (34.61 %), lateral spread (0.16 %), sinkhole (0.03 %), and undefined slope movement (4.72 %).

Visual inspection of Fig. 7 reveals that the zonation obtained adopting the QLR threshold model (maps II in Fig. 7) is more conservative than the zonation obtained using the other two models. In particular, according to the linear model LR (maps I in Fig. 7), 61.9 % of the Italian territory can be considered as non-susceptible. The percentage decreases to 41.6 % for the QNL model (maps III in Fig. 7) and to 21.9 % for the QLR model (maps II in Fig. 7).

To quantify the differences, we intersected the three maps with the GIS layer that portrays the landslide polygons shown in the IFFI database. We computed the proportion of landslide cells that overlaid non-susceptible cells in each map: $I = L_c/N_c \times 100$, where L_c is the number of landslide cells overlaying non-susceptible cells and N_c is the number of landslide cells. This matching index (I) basically corresponds to a False Positive Rate (FPR) that is expressed by the ratio of False Positives (FP) over the sum of True Negatives and False Positives (TN + FP). Since the LR, QLR, and QNL models, and the associated maps (Fig. 7), were obtained using landslide inventories containing mainly translational and rotational slides, earth flows, and complex and compound movements (Cruden and Varnes, 1996), we tested the three models against (i) the entire IFFI inventory, showing all landslide types, and (ii) a subset of the IFFI inventory, showing only translational and rotational slides, earth flows, and complex and compound movements. Results are summarised in Table 2. When the LR linear model is compared to the entire IFFI dataset, a large proportion of the landslide cells is found in non-susceptible cells (I = 43.59 %). The result does not change significantly when the subset is considered (I = 44.02 %). The QLR, and QNL models perform significantly

NHESSD
2, 2813–2849, 2014

better, with comparable values of the matching index when the entire IFFI dataset is used (I = 6.06 % and I = 6.33 % respectively), and when the subset of slides, earth flows, and complex and compound movements is used (I = 5.73 % and I = 5.85 % respectively). We maintain that the QLR model is too conservative, and we conclude that best results are obtained by the QNL model.

The QNL model performed better for translational and rotational slides (Table 3). This was expected, because the 13 inventories used to construct the model shows primarily these landslide types. The value of the matching index for these landslide types (I = 5.3 %) is equivalent to the number of cells that the QNL model leaves below the threshold line (5.3 %). The QNL model failed to detect non-susceptible areas for lateral spreads (I = 20.9 %), sinkholes (13.8 %), and rapid flows (11.6 %). Results improve for slow flows (7.2 %), complex (7.4 %) and undefined (7.2 %) movements, and for falls and topples (8.3 %).

We further investigated the performance of the QNL model in the 20 administrative regions in Italy. Results are summarised in Table 4 that lists, for each region, the I values for two sub-sets of landslides in the IFFI database i.e., (i) translational and rotational slides, slow-moving earth flows, and complex and compound movements, and (ii) translational and rotational slides, and slow-moving earth flows. We focus on the Piemonte, Molise, and Campania Regions (Fig. 2), because (i) they are representative of different terrain an physiographical settings in Italy (Guzzetti and Reichenbach, 1994), (ii) our QNL model was constructed using landslide information outside of these three regions, and (iii) the quality of the landslide information in the IFFI inventory is particularly good in these regions (Trigila et al., 2010). Results indicate that in the Piemonte and the Molise regions the QNL model performed well considering (I = 4.97 % for Piemonte and I = 5.41 % for Molise) and not considering (I = 5.22 % for Piemonte and I = 6.82 % for Molise) the complex and the compound movements. In Campania the model performance was slightly worse (I = 7.30 %, considering the complex and the compound movements, and I = 7.22 %, non considering the complex and compound movements).

NHESSD
2, 2813–2849, 2014

Inspection of Table 4 reveals that in the other regions the performance of the QNL model was also acceptable, with better results obtained not considering the complex and the compound movements. The worst results are obtained by the QNL model in Sardegna (I = 13.84 %, not considering the complex and compound movements), and in Friuli-Venezia Giulia (I = 13.07 %, considering the complex and compound movements). The variation in the performance of the QNL model depends on different terrain conditions and on the quality of the IFFI inventory, which varies significantly in the different regions (Trigila et al., 2010).

We conclude that the QNL model, and the associated terrain zonation (maps III in Fig. 7), is the best among the three prepared models to outline non-susceptible landslide areas i.e., areas where landslide susceptibility is expected to be null or negligible in Italy. We take the QNL model to represent non-susceptible landslide areas in Italy.

5 Non-susceptible areas and the population of Italy

We used map III in Fig. 7 to estimate the proportion of the population of Italy living in areas expected to be non-susceptible to landslides. For the purpose, we used a digital map of the census zones in Italy and the associated population information, distributed by the Italian National Institute of Statistics – ISTAT (http://www.istat.it). The map of the census zones subdivides the Italian territory in a total of 380 000 zones, ranging in size from a few tens of square meters to 325 km^2 (average = 0.8 km^2). The size of the census zones varies: the zones are small to very small in urban areas, large in sub-urban areas, and large to very large in rural and mountain areas. For each census zone, the total number of resident people in 2001 is available.

In the GIS, we first transformed the map of the census zones in Italy to the WGS84 (EPSG 4326) longitude-latitude CRS, and we intersected it with map IIIa in Fig. 7. Next, we classified each census zone based on the proportion of the census zone in non-susceptible areas. We have identified 193 051 census zones where the proportion of non-susceptible areas was 99 %, or larger. These census zones represent 50.5 % of

NHESSD
2, 2813–2849, 2014

the total number of census zones, and cover 20.2 % of the territory covered by census zones in Italy. Some 33.1 million people live in non-susceptible census zones, 57.5 % of the total population of Italy in 2001. We infer that the remaining 42.5 % of the population of Italy lives in areas with some landslide susceptibility. This corresponds to ∼ 24.5 million people.

The total number and the proportion of the population living in non-susceptible areas varies geographically (Table 5). Regions with the largest number of people living in non-susceptible areas include Lombardia, Veneto, Campania, Emilia-Romagna and Puglia, and regions with the largest proportion of people living in non-susceptible areas include Emilia-Romagna (80.65 %), Veneto (79.31 %), Puglia (74.41 %), and Lombardia (73.08 %). These regions host some of the most populated areas in Italy, and some of the largest plains (Guzzetti and Reichenbach, 1994). Regions with the least number of people living in non-susceptible areas are Valle d'Aosta, Liguria, Molise, and Basilicata. The regions where the proportion of the population in susceptible areas is largest are Basilicata (86.35 %), Molise (86.99 %), Liguria (77.35 %), and Valle d'Aosta (74.25 %). In these regions landscape is predominantly mountainous or hilly (Guzzetti and Reichenbach, 1994).

Further inspection of Table 5 reveals no correlation between the total number or the proportion of people living in non-susceptible (or in susceptible areas) and the number of fatal landslide events, the number of landslide fatalities, or the landslide mortality rate in the 50 year period 1963–2012. We explain the lack of relationships with the type of landslides that most frequently cause fatalities in Italy ı.e., rapid to fast-moving rock falls and debris flows (Guzzetti et al., 2005b). These landslide types were not considered in the construction of the QNL model, and the associated terrain zonation (maps III in Fig. 7) used for the analysis. We note that 73 % of the fatal landslide events in Italy in the investigated period occurred outside of the areas classified as non-susceptible in map III of Fig. 7.

NHESSD
2, 2813–2849, 2014

6 Non-susceptibility zonation for the Mediterranean area

The results obtained in Italy are applicable to other geographical areas with similar physiographical and landslide characteristics, and for which the SRTM DEM is available. We applied the non linear model QNL to the landmasses surrounding the Mediterranean Sea (Fig. 1). For each grid cell in the 5 771 205 km^2 area, we used the values of the regional relative relief R and the local terrain slope S to determine if the cell was above or below the QNL threshold model. Grid cells for which the (R, S) pair was below the threshold model were classified as non-susceptible and are shown in red in Fig. 9. Non-susceptible cells cover 3 652 683 km^2, 63 % of the landmasses in the study area. We infer that the other cells, with (R, S) pairs on or above the threshold, covering totally 2 118 521 km^2, (37 %) represent areas with some landslide susceptibility.

We tested the synoptic-scale terrain zonation using independent landslide information in Spain made available to us by the Instituto Geológico y Minero de España – IGME. The landslide dataset was represented by three inventories (N, O, and P in Table 1) for areas in the Pyrenees, Murcia, and the Tramuntana range in Majorca, and comprised a total of 521 landslides with 59 $m^2 < A_L < 1.82$ km^2, an average landslide area A_L = 75 160 m^2, and a total landslide area A_{LT} = 27.24 km^2. Table 1 lists the main characteristics of the landslides of the three inventory maps in Spain.

As performed for Italy, to quantify the geometrical differences between the location of the known landslides in the three inventories and the synoptic zonation of non-susceptible areas (Fig. 9), we computed the fraction of landslide cells L_c that overlaid the non-susceptible cells N_c, $I = L_c/N_c \times 100$, and found I = 6.11 %. The value is slightly larger that the values obtained for Italy, and of the expected proportion of landslide cells in non-susceptible areas (5 %).

Based on the results of the validation performed in Spain, we conclude that the QNL model is adequate to identify zones where landslide susceptibility is expected to be null or negligible in the Mediterranean area (Fig. 9).

NHESSD
2, 2813–2849, 2014

7 Discussion

As pointed out in the Introduction, inspection of the literature revealed that little effort has been made to propose and test methods to assess where landslides are not expected to occur i.e., where landslide susceptibility is null or negligible (Chung and Fabbri, 2003; Fabbri et al., 2003; Godt et al., 2012). This is surprising, because planners and decision makers are equally, or more interested in knowing where landslides are not foreseen, or cannot occur in an area, than knowing where susceptibility is high or very high (Guzzetti et al., 1999; Chung and Fabbri, 2003; Fabbri et al., 2003; Godt et al., 2012). In an attempt to fill this gap, we have proposed a statistically-based method to outline non-susceptible landslide areas i.e., to determine where landslide susceptibility is expected to be negligible in a region. The method produces a synoptic-scale assessment of non-landslide susceptibility for very large regions (Figs. 7 and 9).

Our work showed the importance of landslide information for the production of maps of non-susceptible landslide areas, and confirmed the importance of preparing accurate landslide inventory maps (Guzzetti et al., 2012). Where accurate landslide maps exist, the maps can be used to outline non-susceptible landslide areas in neighbouring and in distant areas. In a recent work, Gunther et al. (2013) have pointed out that a complete coverage of landslide information is not available for Europe, and will not be available in the near future. They further argued that the lack of sufficient landslide information hampers the use of statistical approaches for the definition of continental-scale landslide susceptibility zonations. Our results open to the possibility of using statistical approaches for the synoptic-scale definition on non-susceptible landslide areas, provided accurate landslide information is available for some areas. Determining the minimum amount and quality (Guzzetti et al., 2012) of the landslide information required for reliable statistical zonations of non-susceptible landslide areas remains an open problem.

NHESSD
2, 2813–2849, 2014

The new method produces geographical assessments of non-susceptible landslide areas for very large regions (Figs. 7 and 9). The quality and geographical resolution of the terrain zonation depend on the quality and resolution of the terrain information used to calibrate and apply the model. The two morphometric variables used in this study were local terrain slope and regional relative relief. It is known that the accuracy of morphometric derivatives of elevation data depend on the resolution of the DEM. Use of higher resolution DEMs (e.g., the 10 m-resolution TINITALY/01 DEM of Italy Tarquini et al., 2007, 2012) would have probably increased the accuracy of the slope and, subordinately, of the relative relief measurements. However, use of the higher resolution DEM would have not allowed to apply the model to the wider Mediterranean area (Fig. 9), for which the TINITALY/01 DEM is not available.

The method produces synoptic-scale zonations that cannot be used to ascertain the susceptibility (or the lack of susceptibility) of single sites. For the purpose, more accurate, site-specific analyses must be performed. In the non-susceptible areas, landslide susceptibility is expected to be null or negligible i.e., a few landslides can occur in the non-susceptible areas. This has two reasons. First, the quantile non linear model QNL was constructed to have a proportion of the (R, S) empirical points representing landslide cells below the threshold model. Second, landslides may originate in susceptible areas and travel significant distances to deposit in non-susceptible areas. These landslide types include e.g., rock fall, debris flow, and lateral spread. In a few places, the proposed method outlined non-susceptible areas inside very large landslide deposits. Reasons for the (apparent) discrepancy include the fact that large, deep-seated landslides can produce significant patches of "flat" terrain in the depletion zone and in the toe area of the landslides, and that very large landslides are very old and partially dismantled by erosion and other landslides. We cannot exclude the possibility that the proposed model has failed to capture local terrain instability conditions.

NHESSD
2, 2813–2849, 2014

8 Conclusions

Exploiting accurate landslide information for 13 study areas in Italy, collectively covering 8.9 % of the Italian territory, and topographic information obtained from the SRTM DEM, version 2.1, we identified areas non-susceptible to landslides in Italy i.e., areas where landslide susceptibility is null or negligible. In these areas, collectively covering 41.6 % of Italy, landslides are not expected. We infer that in the remaining part of Italy, 58.4 %, some level of landslide susceptibility is expected.

We used the map showing the areas expected to be non-susceptible to landslides in Italy, and a map of the census zones in Italy, to determine the location and the total number of people living in non-susceptible landslide areas. We found that 57.5 % of the population of Italy (33.1 million people) live in non-susceptible areas, and we infer that the remaining 42.5 % (24.5 million people) live in areas with some susceptibility to landslides.

We extended the application of the non-susceptibility model to a 5.8×10^6 km^2 area surrounding the Mediterranean Sea, and we tested the synoptic subdivision using independent landslide information for three areas in Spain. Results proved that or model was capable of determining where landslide susceptibility is expected to be null or negligible in the Mediterranean area.

We expect that our synoptic-scale zonation for Italy and for the landmasses surrounding the Mediterranean Sea can be used for insurance and re-insurance purposes (Godt et al., 2012), for small-scale land planning, and in operational landslide warning systems (Brunetti et al., 2009; Rossi et al., 2012) to outline areas where landslides are not expected, regardless of the trigger.

NHESSD
2, 2813–2849, 2014

Acknowledgements. Work supported by the Italian Department for Civil Protection, and by a grant of the Fondazione Assicurazioni Generali, Trieste. MA was supported by a grant of the Regione Umbria, under contract *POR-FESR Umbria 2007–2013, asse ii, attività a1, azione 5*, and by the *Dipartimento della Protezione Civile*, Italy. We thank G. Herrera Garcia and R. M. Mateos (IGME) for making available landslide data for three study areas in Spain, and P. Salvati (CNR IRPI) for providing updated figures on the number of fatal landslides and of landslides fatalities in Italy in the period 1963–2012.

References

Antonini, G., Cardinali, M., Guzzetti, F., Reichenbach, P., and Sorrentino, A.: Carta Inventario dei Fenomeni Franosi della Regione Marche ed aree limitrofe, CNR Gruppo Nazionale per la Difesa dalle Catastrofi Idrogeologiche Publication n. 580, 2 sheets, scale 1 : 100,000, 1993 (in Italian). 2816, 2817, 2836

Antonini, G., Ardizzone, F., Cardinali, M., Carrara, A., Detti, R., Galli, M., Guzzetti, F., Reichenbach, P., Sotera, M., Tonelli, G.: Rapporto Finale, Convenzione fra il CNR, IRPI di Perugia e CSITE di Bologna, e la Regione Lombardia, Direzione Generale al Territorio ed Edilizia Residenziale, per lo sviluppo di tecniche e metodologie idonee alla produzione di carte della pericolositá e del rischio da frana in aree campione rappresentative del territorio della Regione Lombardia, unpublished report, 120 pp., 2000, (in Italian). 2816, 2817, 2836, 2844

Antonini, G., Ardizzone, F., Cacciano, M., Cardinali, M., Castellani, M., Galli, M., Guzzetti, F., Reichenbach, P., and Salvati, P.: Rapporto Conclusivo, Protocollo di Intesa fra la Regione dell'Umbria, Direzione Politiche Territoriali Ambiente e Infrastrutture, ed il CNR IRPI di Perugia per l'acquisizione di nuove informazioni sui fenomeni franosi nella regione dell'Umbria, la realizzazione di una nuova carta inventario dei movimenti franosi e dei siti colpiti da dissesto, l'individuazione e la perimetrazione delle aree a rischio da frana di particolare rilevanza, e l'aggiornamento delle stime sulla incidenza dei fenomeni di dissesto sul tessuto insediativo, infrastrutturale e produttivo regionale, unpublished report, 140 pp., 2002 (in Italian). 2816, 2817, 2836

Ardizzone, F., Cardinali, M., Galli, M., Guzzetti, F., and Reichenbach, P.: Identification and mapping of recent rainfall-induced landslides using elevation data collected by airborne Lidar, Nat. Hazards Earth Syst. Sci., 7, 637–650, doi:10.5194/nhess-7-637-2007, 2007. 2816

NHESSD

2, 2813–2849, 2014

Ardizzone, F., Basile, G., Cardinali, M., Casagli, N., Del Conte, S., Del Ventisette, C., Fiorucci, F., Garfagnoli, F., Gigli, G., Guzzetti, F., Iovine, G. G. R., Mondini, A. C., Moretti, S., Panebianco, M., Raspini, F., Reichenbach, P., Rossi, M., Tanteri, L., and Terranova, O.: Landslide inventory map for the Briga and the Giampilieri catchments, NE Sicily, Italy, J. Maps, 8, 176–180, doi:10.1080/17445647.2012.694271, 2012. 2816, 2817, 2836

Brabb, E. E.: Innovative approaches to landslide hazard and risk mapping, in: Proceedings of the 4th International Symposium on Landslides, Toronto, Canada, 1, 30–32, 1984. 2814

Brunetti, M. T., Peruccacci, S., Rossi, M., Guzzetti, F., Reichenbach, P., Ardizzone, F., Cardinali, M., Mondini, A. C., Salvati, P., and Tonelli, G.: A prototype system to forecast rainfall induced landslides in Italy, in: Proceedings of the First Italian Workshop on Landslides, 2009. 2830

Cardinali, M., Ardizzone, F., Galli, M., Guzzetti, F., and Reichenbach, P.: Landslides triggered by rapid snow melting: the December 1996–January 1997 event in Central Italy, in: Proceedings 1st Plinius Conference, edited by: Claps, P. and Siccardi, F., Maratea. Bios Publisher, Cosenza, 439–448, 2000. 2816, 2836

Cardinali, M., Antonini, G., Reichenbach, P., and Guzzetti, F.: Photo-geological and landslide inventory map for the Upper Tiber River basin, CNR Gruppo Nazionale per la Difesa dalle Catastrofi Idrogeologiche Publication n. 2116, scale 1 : 100,000, 2001. 2816, 2817, 2836

Chung, C.-J. F. and Fabbri, A. G.: Probabilistic prediction models for landslide hazard mapping, ISPRS J. Photogramm., 65, 1389–1399, 1999. 2815

Chung, C.-J. F. and Fabbri, A. G.: Validation of spatial prediction models for landslide hazard mapping, Nat. Hazards, 30, 451–472, 2003. 2815, 2828

Cruden, D. M. and Varnes, D. J.: Landslide types and processes. in: Landslides, Investigation and Mitigation, edited by: Turner, A. K. and Schuster, R. L., Special Report 247, Transportation Research Board, Washington DC, 36–75, ISBN: 030906208 X, 1996. 2817, 2823

De La Beaujardiere, J.: OGC Web Map Service Interface, version 1.3. 0. Open Geospatial Consortium, available at: http://www.opengeospatial.org/standards/wms, 2004. 2822

Farahmand, A. and AghaKouchak, A.: A satellite-based global landslide model, Nat. Hazards Earth Syst. Sci., 13, 1259–1267, doi:10.5194/nhess-13-1259-2013, 2013. 2815

Fabbri, A. G., Chung, C.-J. F., Cendrero, A., and Remondo, J.: Is prediction of future landslides possible with a GIS?, Nat. Hazards, 30, 487–503, 2003. 2815, 2828

Farr, T. G., Rosen, P. A., Caro, E., Crippen, R., Duren, R., Hensley, S., Kobrick, M., Paller, M., Rodriguez, E., Roth, L., Seal, D., Shaffer, S., Shimada, J., Umland, J., Werner, M., Oskin,

NHESSD
2, 2813–2849, 2014

M., Burbank, D., and Alsdorf, D.: The Shuttle Radar Topography Mission, Rev. Geophys., 45, RG2004, doi:10.1029/2005RG000183, 2007. 2816

Galli, M., Ardizzone, F., Cardinali, M., Guzzetti, F., and Reichenbach, P.,: Comparing landslide inventory maps, Geomorphology, 94, 268–289, 2008. 2816, 2817, 2836

Godt, J. W., Coe, J. A., Baum, R. L., Highland, L. M., Keaton, J. R., and Roth Jr., R. J.: Prototype landslide hazard map of the conterminous United states, in: Landslides and Engineered Slopes: Protecting Society through Improved Understanding, edited by: Eberhardt, E., Froese, C., Turner, K., and Leroueil, S., Taylor & Francis Group, London, ISBN 978-0-415-62123-6, 2012. 2815, 2816, 2817, 2818, 2819, 2820, 2828, 2830

Gunther, A., Reichenbach, P., Malet, J. P., Van Den Eeckhaut, M., Hervás, J., Dashwood, C., and Guzzetti, F.: Tier-based approaches for landslide susceptibility assessment in Europe, Landslides, 10, 529–546, doi:10.1007/s10346-012-0349-1, 2011. 2815, 2828

Guzzetti, F.: Landslide Hazard and Risk Assessment, Ph.D. thesis, Mathematich-Naturwissenschaftlichen Fakultät, Rheinischen Friedrich-Wilhelms-Universitat Bonn, 389 pp., 2005. 2815

Guzzetti, F. and Reichenbach, P.: Towards a definition of topographic divisions for Italy, Geomorphology, 11, 57–74, 1994. 2817, 2824, 2826

Guzzetti, F., Carrara, A., Cardinali, M., and Reichenbach, P.: Landslide hazard evaluation: a review of current techniques and their application in a multi-scale study, Central Italy, Geomorphology, 31, 181–216, 1999. 2815, 2828

Guzzetti, F., Cardinali, M., Reichenbach, P., Cipolla, F., Sebastiani, C., Galli, M., and Salvati, P.: Landslides triggered by the 23 November 2000 rainfall event in the Imperia Province, Western Liguria, Italy, Eng. Geol., 73, 229–245, 2004. 2816, 2817, 2836

Guzzetti, F., Reichenbach, P., Cardinali, M., Galli, M., and Ardizzone, F.: Probabilistic landslide hazard assessment at the basin scale, Geomorphology, 72, 272–299, 2005a. 2815, 2816, 2817, 2836

Guzzetti, F., Stark, C. P., and Salvati, P.: Evaluation of flood and landslide risk to the population of Italy, Environ. Manage., 36, 15–36, doi:10.1007/s00267-003-0257-1, 2005b. 2826

Guzzetti, F., Galli, M., Reichenbach, P., Ardizzone, F., and Cardinali, M.: Landslide hazard assessment in the Collazzone area, Umbria, Central Italy, Nat. Hazards Earth Syst. Sci., 6, 115–131, doi:10.5194/nhess-6-115-2006, 2006. 2816, 2817, 2836

NHESSD

2, 2813–2849, 2014

Guzzetti, F., Ardizzone, F., Cardinali, M., Rossi, M., and Valigi, D.: Landslide volumes and landslide mobilization rates in Umbria, central Italy, Earth Planet. Sc. Lett., 279, 222–229, doi:10.1016/j.epsl.2009.01.005, 2009. 2816, 2817, 2836

Guzzetti, F., Mondini, A. C., Cardinali, M., Fiorucci, F., Santangelo, M., and Chang, K.-T.: Landslide inventory maps: new tools for and old problem, Earth-Sci. Rev., 112, 42–66, doi:10.1016/j.earscirev.2012.02.001, 2012. 2815, 2828

Hong, Y., Adler, R., and Huffman, G.: Use of satellite remote sensing data in the mapping of global landslide susceptibility, Nat. Hazards, 43, 245–256, 2007a. 2815

Hong, Y., Adler, R., and Huffman, G.: An experimental global prediction system for rainfall-triggered landslides using satellite remote sensing and geospatial datasets, IEEE T. Geosci. Remote, 45, 1671–1680, 2007b. 2815

Horn, B. K. P.: Hill shading and the reflectance map, P. IEEE, 69, 14–47, 1981. 2819

Jarvis, A., Reuter, H. I., Nelson, A., and Guevara, E.: Hole-filled seamless SRTM data V4, International Centre for Tropical Agriculture (CIAT), available from http://srtm.csi.cgiar.org, 2008. 2816

Koenker, R. W.: Quantile Regression, Cambridge U. Press, 2005. 2821

Kirschbaum, D. B., Adler, R., Hong, Y., and Lerner-Lam, A.: Evaluation of a preliminary satellite-based landslide hazard algorithm using global landslide inventories, Nat. Hazards Earth Syst. Sci., 9, 673–686, doi:10.5194/nhess-9-673-2009, 2009. 2815

Nadim, F., Kjekstad, O., Peduzzi, P., Herold, C., and Jaedicke, C.: Global landslide and avalanche hotspots, Landslides, 3, 159–173, 2006. 2815

Rossi, M., Peruccacci, S., Brunetti, M. T., Marchesini, I., Luciani, S., Ardizzone, F., Balducci, V., Bianchi, C., Cardinali, M., Fiorucci, F., Mondini, A. C., Reichenbach, P, Salvati, P., Santangelo, M., Bartolini, D., Gariano, S. L., Palladino, M., Vessia, G., Viero, A., Antronico, L., Borselli, L., Deganutti, A. M., Iovine, G., Luino, F., Parise, M., Polemio, M., Tonelli, G., Guzzetti, F.: SANF: national warning system for rainfall-induced landslides in Italy, in: Landslides and Engineered Slopes: Protecting Society through Improved Understanding, edited by: Eberhardt, E., Froese, C., Turner, A. K., and Leroueil, S., vol. 2, 1895–1899, 2012. 2830

Salvati, P., Bianchi, C., Rossi, M., and Guzzetti, F.: Societal landslide and flood risk in Italy, Nat. Hazards Earth Syst. Sci., 10, 465–483, doi:10.5194/nhess-10-465-2010, 2010.

Tarquini, S., Isola, I., Favalli, M., Mazzarini, F., Bisson, M., Pareschi, M. T., and Boschi, E.: TINITALY/01: a new Triangular Irregular Network of Italy, Ann. Geophys.-Italy, 50, 407–425, doi:10.4401/ag-4424 2007. 2829

NHESSD

2, 2813–2849, 2014

Tarquini, S., Vinci, S., Favalli, M., Doumaz, F., Fornaciai, A., and Nannipieri, L.: Release of a 10-m-resolution DEM for the Italian territory: comparison with global-coverage DEMs and anaglyph-mode exploration via the web, Comput. Geosci., 38, 168–170, 2012. 2829

Trigila, A., Iadanza, C., and Spizzichino, D.: Quality assessment of the Italian landslide inventory using GIS processing, Landslides, 7, 455–470, doi:10.1007/s10346-010-0213-0, 2010. 2822, 2824, 2825, 2838, 2839

Van Den Eeckhaut, M., Hervás, J., Jaedicke, C., Malet, J. P., Montanarella, L., and Nadim, F.: Statistical modelling of Europe-wide landslide susceptibility using limited landslide inventory data, Landslides, 9, 357–369, 2012. 2815

Verdin, K. L., Godt, J., Funk, C., Pedreros, D., Worstell, B., and Verdin, J.: Development of a global slope dataset for estimation of landslide occurrence resulting from earthquakes, US Geological Survey Open-File Report 2007-1188, 2007. 2816

NHESSD

2, 2813–2849, 2014

Table 1. Information on the landslide inventory maps used in this work. See Fig. 2 for the location of the inventory maps. (A) Umbria region, central Italy. (B) Collazone, Umbria, central Italy. (C) Upper Tiber River basin, central Italy. (D) Marche, central Italy. (E) Basento and Cavone catchments, southern Italy. (F) Staffora catchment, Lombardia, northern Italy. (G) Setta catchment, Emilia-Romagna, northern Italy. (H) Messina, Sicilia, southern Italy. (I) Lunigiana, Toscana, northern Italy. (J) Lecco, Lombardia, northern Italy. (K) Valcamonica, Lombardia, northern Italy. (L) Valseriana, Lombardia, northern Italy. (M) Imperia, Liguria, northern Italy. (N) Pyrenees, northern Spain. (O) Murcia, southern Spain. (P) Tramuntana range, Majorca, Spain. Legend: GM, geomorphological landslide inventory map; EV, event landslide inventory map; MT, multi-temporal landslide inventory map; na information not available; u unpublished map. References: [1] Antonini et al. (2002), [2] Cardinali et al. (2000), [3] Guzzetti et al. (2006); Galli et al. (2008); Guzzetti et al. (2009), [4] Cardinali et al. (2001), [5] Antonini et al. (1993), [6] Guzzetti et al. (2005a), [7] Ardizzone et al. (2012), [8] Antonini et al. (2000), [9] Guzzetti et al. (2004), [10] G. Herrera Garcia and R. M. Mateos, personal communication, 2013.

ID	Study area		Inventory	Landslide		Min area	Max area	Mean area	Scale		Source
	Name	km^2	Type	#	[km^2]	[m^2]	[m^2]	[m^2]	Aerial photographs	Map	
A	Umbria	8,456	GM	44 039	545	70	1 847 000	12 382	1 : 33k, 1 : 13k, 1 : 73k	1 : 10k	[1]
		1,500	EV	4,234	13	40	151 476	2,998	1 : 20k	1 : 10k	[2]
B	Collazzone	80	MT	2,849	11	36	75 256	3,923	1 : 13k to 1 : 33k	1 : 10k	[3]
C	Upper Tiber River	4,098	GM	16 731	364	170	1 081 650	21 751	1 : 33k, 1 : 13k	1 : 25k	[4]
D	Marche	9,366	GM	8,713	880	2,711	4 382 960	100 642	1 : 33k	1 : 25k	[5]
E	Basento &Cavone	1,411	GM	1,843	167	2,554	3 676 040	90 643	1 : 33k	1 : 25k	u
F	Staffora	274	MT	3,746	187	145	178 735	49 862	1 : 15k to 1 : 40k	1 : 10k	[6]
G	Setta	317	GM	847	63	437	1 403 270	74 591	na	na	u
H	Messina	2,326	GM	6,293	288	107	3 875 534	46 524	1 : 29 to 1 : 33k	na	u
		19	EV	31	0.05	39	21 918	1,654	1 : 3500, 1 : 4500	1 : 10k	[7]
I	Lunigiana	358	GM	140	59	15 705	7 261 520	419 799	1 : 33k, 1 : 20k	1 : 10k	u
J	Lecco	605	GM	1,449	13	21	2 094 960	8,823	na	na	[8]
K	Valcamonica	1,449	GM	980	94	118	2 684 700	95 920	na	na	[8]
L	Valseriana	269	GM	249	24	1,435	1 566 490	94 936	na	na	[8]
M	Imperia	500	GM	626	17	105	335 885	26 791	1 : 55k	1 : 10k	[9]
			EV	768	0.7	50	72 580	868	1 : 13k, 1 : 5k	1 : 10k	
N	Pyrenees	68	GM	255	14	155	1 062 860	56 025	na	na	[10]
O	Mallorca	1,282	GM	228	12	60	1 824 280	53 773	na	na	[10]
P	Murcia	12	GM	36	0.6	273	131 732	16 834	na	na	[10]

NHESSD
2, 2813–2849, 2014

Table 2. Proportion of landslide cells shown in the IFFI database in non-susceptible cells classified by three models: LR linear model, Eq. (6), quantile linear model QLR model, Eq. (7), and QNL quantile non linear model, Eq. (8). See text for explanation.

All landslide types			
Model	LR [%]	QLR [%]	QNL [%]
	43.59	6.06	6.33

Slide, earth flow, complex and compound movement			
Model	LR [%]	QLR [%]	QNL [%]
	44.02	5.73	5.85

NHESSD
2, 2813–2849, 2014

Table 3. Values of the *I* matching index for the QNL model, for different types of landslides shown in the IFFI database (Trigila et al., 2010). See text for explanation.

Landslide type	I [%]
Fall and topple	8.3
Slow flow	7.2
Complex and compound movement	7.4
Rapid flow	11.6
Translation and rotational slide	5.3
Undefined	7.2
Lateral spread	20.9
Sinkhole	13.8

NHESSD
2, 2813–2849, 2014

Table 4. Values of the *I* matching index obtained comparing the QNL model (Map III in Fig. 7) with landslides shown in the IFFI database (Trigila et al., 2010), for different administrative regions in Italy. (A) landslide subset comprising slides, earth flows, and complex and compound movement. (B) landslide subset comprising slides and earth flows. See text for explanation.

Region	A [%]	B [%]
Piemonte	5.22	4.97
Lombardia	5.30	4.05
Veneto	6.33	6.21
Liguria	3.61	3.89
Emilia-Romagna	5.55	6.02
Toscana	5.37	5.66
Umbria	5.32	5.30
Marche	6.37	5.70
Lazio	9.33	11.10
Abruzzo	5.24	5.57
Molise	6.82	5.41
Campania	7.22	7.30
Puglia	8.18	9.22
Basilicata	4.90	4.87
Calabria	4.90	4.85
Sicilia	7.66	7.49
Sardegna	10.11	13.84
Valle d'Aosta	7.12	5.54
Trentino-Alto Adige	11.43	6.74
Friuli-Venezia Giulia	13.07	10.22

NHESSD
2, 2813–2849, 2014

Table 5. Number and percentage of peoples living in areas where landslide susceptibility is expected to be null or negligible in Italy.

Region	Non-susceptibile area [%]	Citizens in non-susceptible area [#]	Citizens in non-susceptible area [%]	Fatal landslides (1963–2012) [#]	Landslide fatalities (1963–2012) [#]	Landslide mortality (1963–2012)
Molise	23.28	334 133	13.01	2	4	0.023
Basilicata	26.92	616 347	13.65	7	18	0.058
Liguria	9.35	1 587 826	22.65	16	37	0.042
Calabria	25.10	2 034 604	24.08	19	38	0.037
Valle d'Aosta	12.55	119 632	25.75	12	25	0.423
Abruzzo	22.95	1 291 394	27.82	7	9	0.014
Marche	22.03	1 543 531	27.87	9	11	0.016
Trentino-Alto Adige	13.03	943 414	34.09	54	355	0.810
Umbria	28.00	850 604	36.00	8	15	0.038
Sicilia	34.38	4 968 991	40.32	21	70	0.083
Sardegna	41.49	1 631 880	49.02	11	15	0.028
Lazio	45.33	5 144 187	47.72	15	24	0.010
Toscana	30.95	3 551 049	57.23	30	68	0.039
Campania	34.63	5 787 348	58.04	96	306	0.111
Piemonte	42.15	4 233 649	62.98	52	137	0.063
Friuli-Venezia Giulia	53.13	1 212 343	65.97	9	223	0.370
Lombardia	59.54	9 077 266	73.08	40	123	0.028
Puglia	82.67	4 042 899	74.41	6	12	0.006
Veneto	66.39	4 611 136	79.14	26	1780	0.914
Emilia-Romagna	56.21	4 052 909	80.65	2	49	0.025

NHESSD
2, 2813–2849, 2014

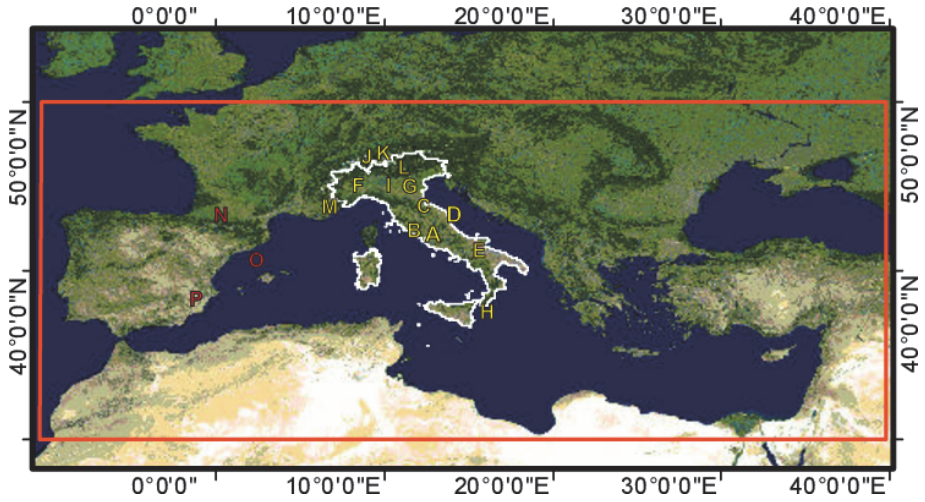

Fig. 1. Location of the study areas. White line shows Italy, where the non-susceptibility landslide model was calibrated, and tested. Red box shows the area surrounding the Mediterranean Sea, where the model was applied. Yellow capital letters (A to M) show locations of the landslide inventories used to calibrate and red capital letters (N to P) other locations used to validate the non-susceptibility model. Legend: (A) Umbria region, central Italy. (B) Collazone, Umbria, central Italy. (C) Upper Tiber River basin, central Italy. (D) Marche, central Italy. (E) Basento and Cavone catchments, southern Italy. (F) Staffora catchment, Lombardia, northern Italy. (G) Setta catchment, Emilia-Romagna, northern Italy. (H) Messina, Sicilia, southern Italy. (I) Lunigiana, Toscana, northern Italy. (J) Lecco, Lombardia, northern Italy. (K) Valcamonica, Lombardia, northern Italy. (L) Valseriana, Lombardia, northern Italy. (M) Imperia, Liguria, northern Italy. (N) Pyrenees, northern Spain (O) Murcia, southern Spain. (P) Tramuntana range, Majorca, Spain. See Table 1 for details on the study areas and the landslide inventories.

NHESSD
2, 2813–2849, 2014

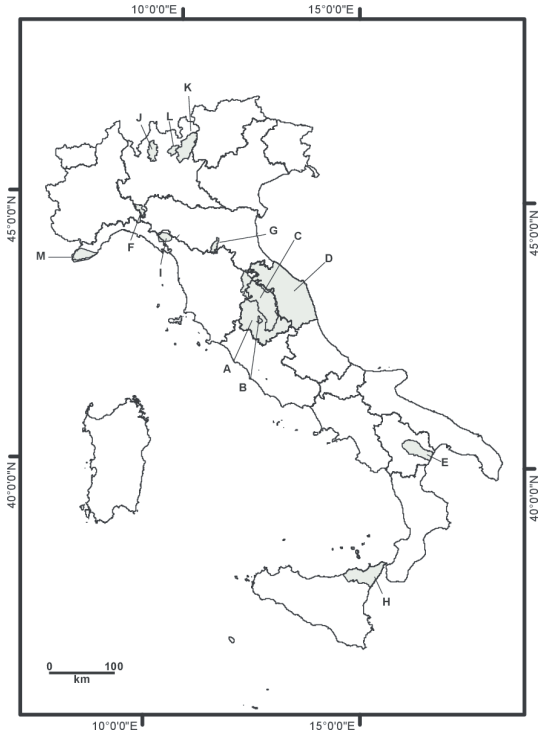

Fig. 2. Location and areal extent of the 13 landslide inventory maps in Italy used in this study. Legend: (A) Umbria region, central Italy. (B) Collazone, Umbria, central Italy. (C) Upper Tiber River basin, central Italy. (D) Marche, central Italy. (E) Basento and Cavone catchments, southern Italy. (F) Staffora catchment, Lombardia, northern Italy. (G) Setta catchment, Emilia-Romagna, northern Italy. (H) Messina, Sicilia, southern Italy. (I) Lunigiana, Toscana, northern Italy. (J) Lecco, Lombardia, northern Italy. (K) Valcamonica, Lombardia, northern Italy. (L) Valseriana, Lombardia, northern Italy. (M) Imperia, Liguria, northern Italy. See Table 1 for details on the study areas and the landslide inventories.

NHESSD
2, 2813–2849, 2014

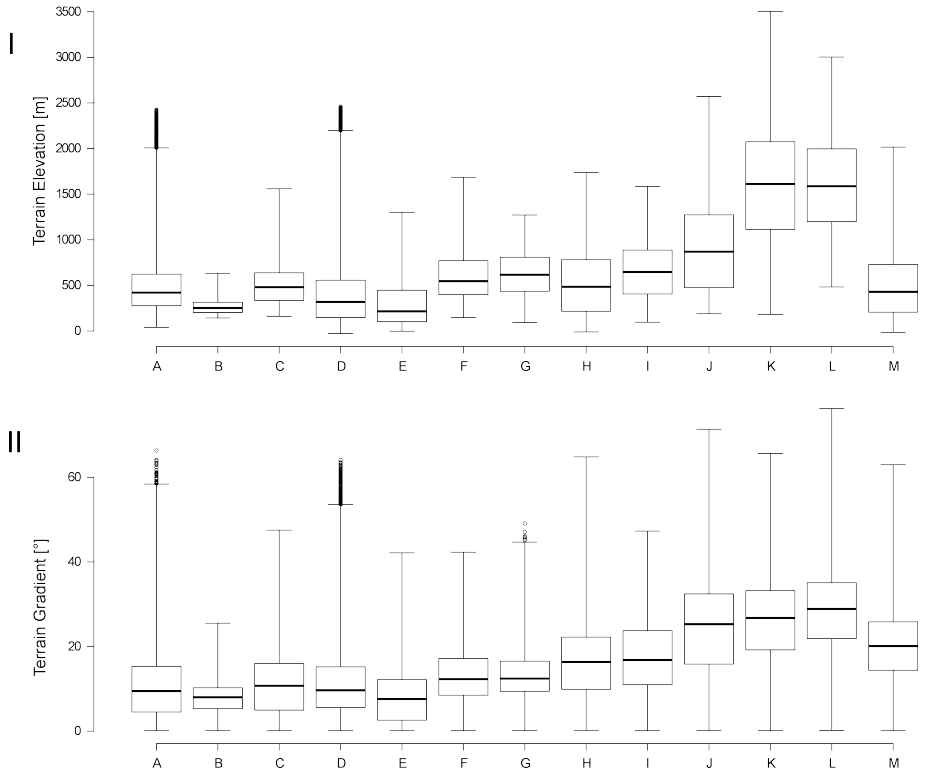

Fig. 3. Terrain morphology in the 13 areas in Italy for which landslide inventories were available to us. See Fig. 2 for the location of the areas. Box plots show the distributions of (upper chart) terrain elevation and (lower chart) terrain gradient. The whiskers extend to the most extreme data point which is no more than 4 times the interquartile range from the box. Legend: (A) Umbria, (B) Collazone, (C) Upper Tiber River, (D) Marche, (E) Basento and Cavone, (F) Staffora, (G) Setta, (H) Messina, (I) Lunigiana, (J) Lecco, (K) Valcamonica, (L) Valseriana, (M) Imperia. See Table 1 for details on the study areas and the inventory maps, and Fig. 2 for the location of the areas.

NHESSD
2, 2813–2849, 2014

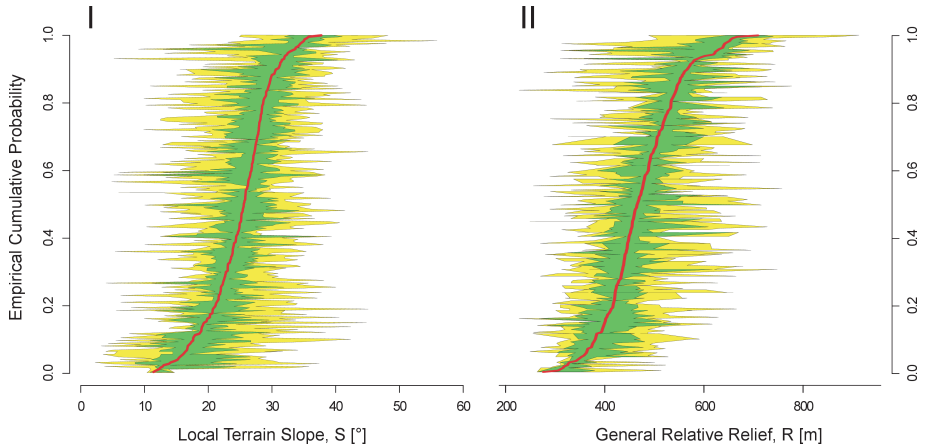

Fig. 4. Empirical Cumulative Distribution Function (ECDF) of (I) local terrain slope *S* and (II) regional relative relief *R* computed for each landslide shown in the Valcamonica inventory map, L in Table 1 (Antonini et al., 2000). Red line shows ECDF for the median (50th percentile), green area shows 25th–75th percentile range, yellow area shows 5th–95th percentile range.

NHESSD
2, 2813–2849, 2014

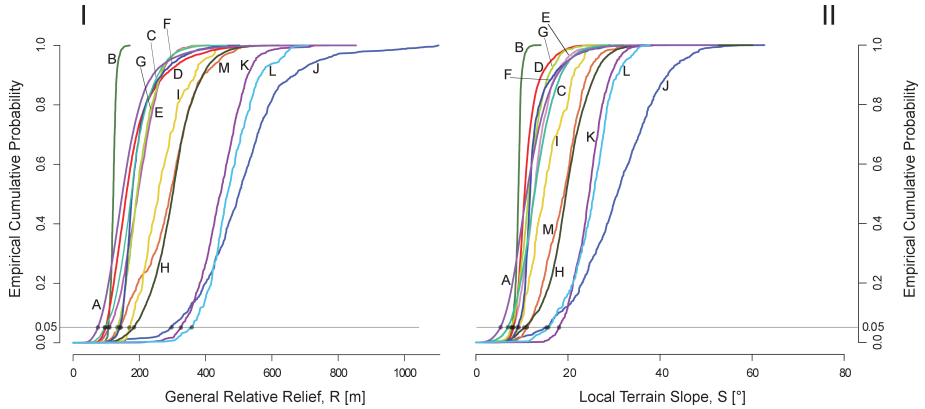

Fig. 5. Empirical Cumulative Distribution Functions (ECDFs) for the median (50th percentile) of the values of the regional relative relief R and the local terrain slope S, for the 13 landslide inventories. Horizontal lines show 5 % values of R_{50} and S_{50}. Black dots along the horizontal lines represent the empirical R_{50} and S_{50} values used to prepare Fig. 6. Legend: (A) Umbria, (B) Collazone, (C) Upper Tiber River, (D) Marche, (E) Basento and Cavone, (F) Staffora, (G) Setta, (H) Messina, (I) Lunigiana, (J) Lecco, (K) Valcamonica, (L) Valseriana, (M) Imperia. See Table 1 for details on the study areas and the inventory maps, and Fig. 2 for the location of the areas.

NHESSD
2, 2813–2849, 2014

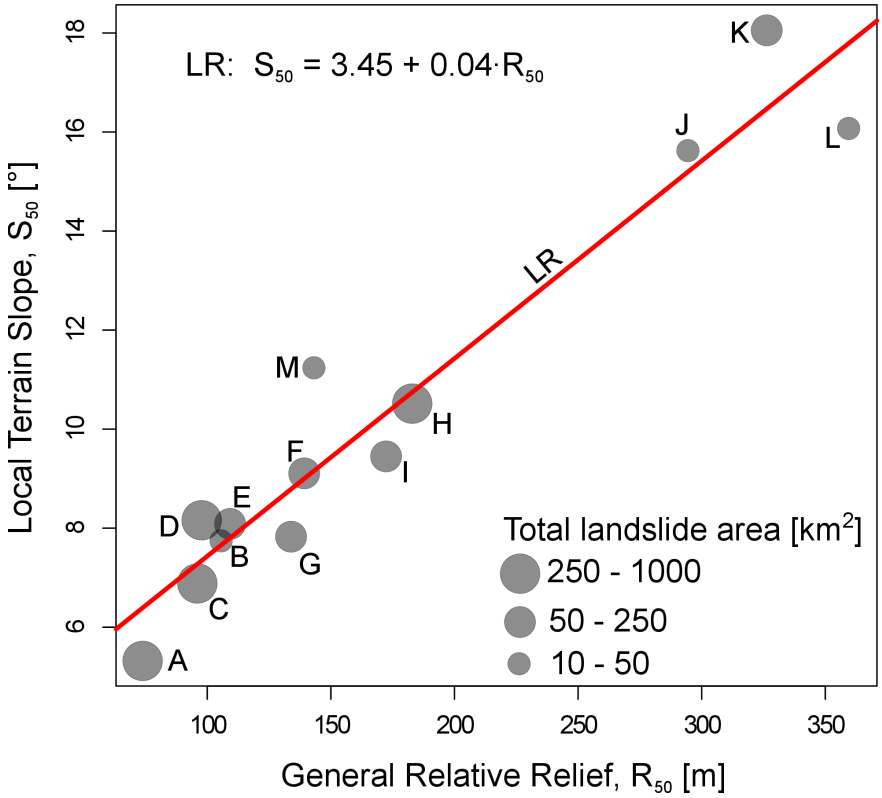

Fig. 6. Plot of the 5th percentiles for the Empirical Cumulative Distribution Function (ECDF) for the median of local terrain slope S_{50} and general relative relief R_{50}. Re line represents best linear fit LR (Eq. 6). Increasing number of landslides in the inventory is shown by symbols of increasing size. Legend: (A) Umbria, (B) Collazone, (C) Upper Tiber River, (D) Marche, (E) Basento and Cavone, (F) Staffora, (G) Setta, (H) Messina, (I) Lunigiana, (J) Lecco, (K) Valcamonica, (L) Valseriana, (M) Imperia. See Table 1 for details on the study areas and the inventory maps, and Fig. 2 for the location of the areas.

NHESSD
2, 2813–2849, 2014

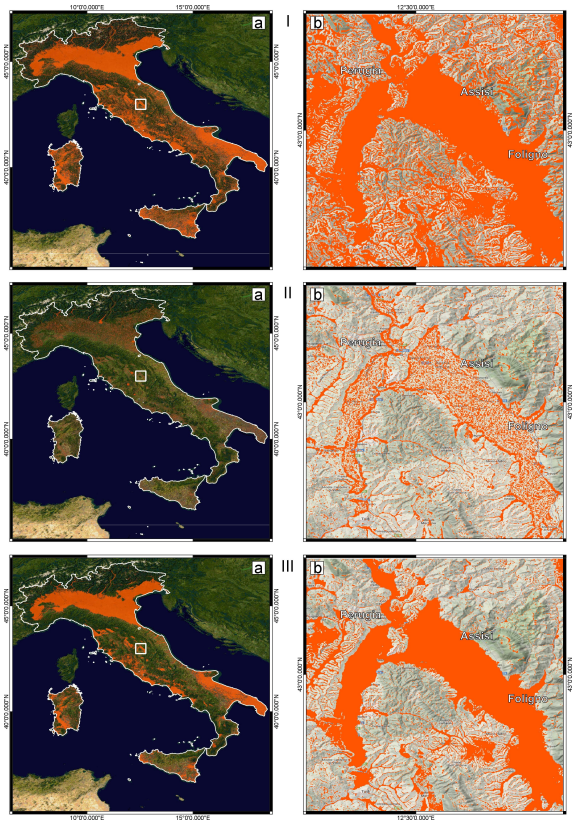

Fig. 7. Maps showing zonations of non-susceptible landslide areas in Italy. Red colour shows non-susceptible areas, and other colours show terrain outside non-susceptible landslide areas. (Ia) Map prepared adopting method I, Eq. (6). (IIa) Map prepared adopting method II, Eq. (7). (IIIa) Map prepared adopting method II, Eq. (8). Insets (Ib, IIb, IIIb) show enlargements for a portion of study area in Umbria, central Italy. See text for explanation. Background images of insets: ©2013 Google.

NHESSD
2, 2813–2849, 2014

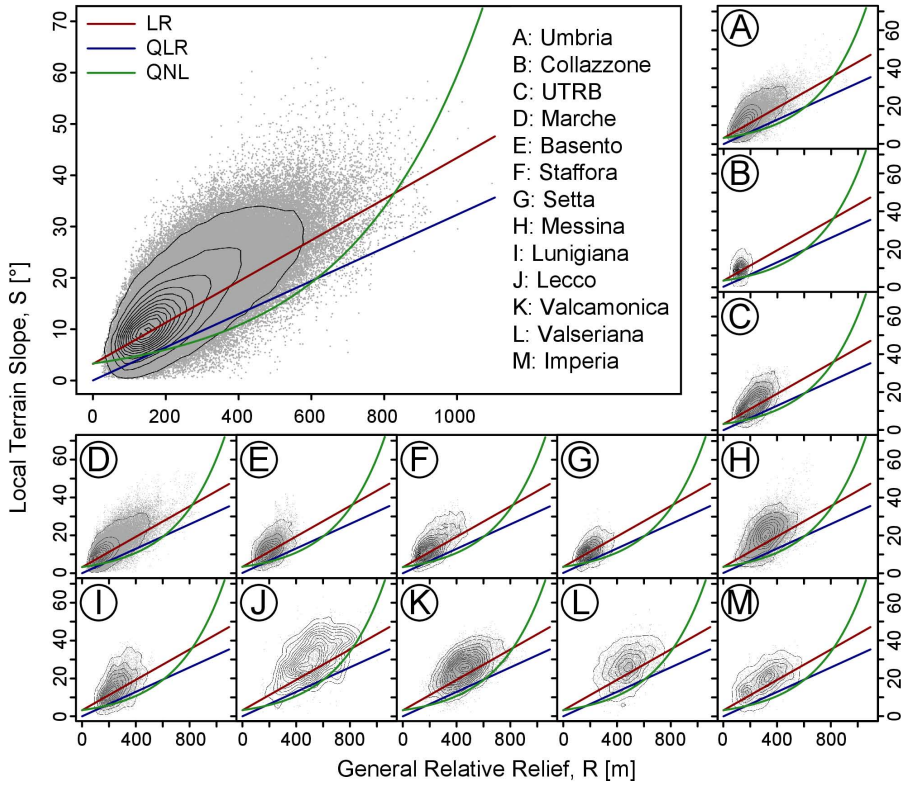

Fig. 8. Plots show relative relief *R* (x-axis) and terrain slope *S* computed for all grid cells in all landslides shown in the 13 inventory maps used in this study (Fig. 2). Red line shows LR model, Eq. (6). Blue line shows QLR model, Eq. (7). Green line shows QNL model, Eq. (8). See text for explanation. Legend: (A) Umbria, (B) Collazone, (C) Upper Tiber River, (D) Marche, (E) Basento and Cavone, (F) Staffora, (G) Setta, (H) Messina, (I) Lunigiana, (J) Lecco, (K) Valcamonica, (L) Valseriana, (M) Imperia. See Table 1 for details on the study areas and the inventory maps, and Fig. 2 for the location of the areas.

NHESSD
2, 2813–2849, 2014

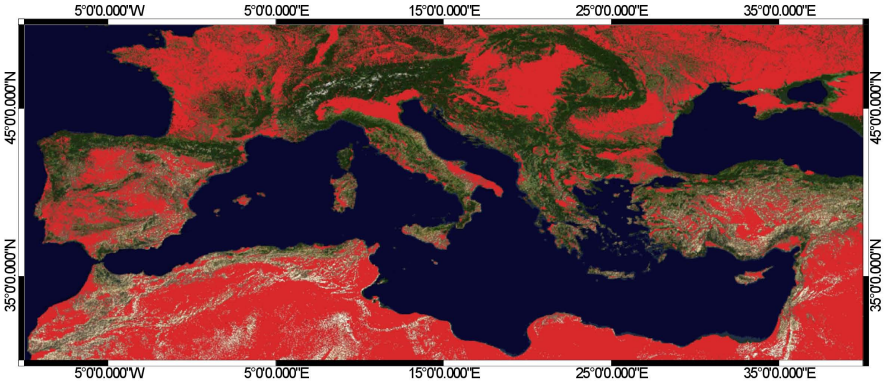

Fig. 9. Map showing zonation of non-susceptible landslide for the landmasses surrounding the Mediterranean Sea. Red shows non-susceptible areas, and other colours show terrain outside non-susceptible areas. Zonation was obtained using the QNL model, Eq. (8). See text for explanation.

NHESSD
2, 2813–2849, 2014